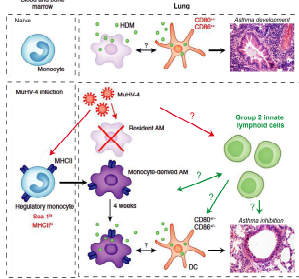


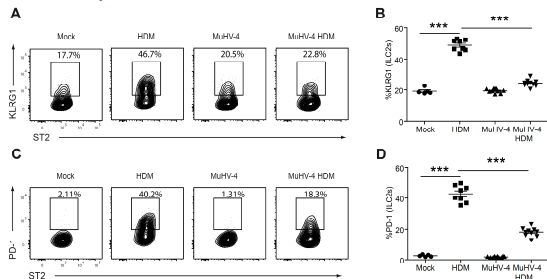
The “Hygiene hypothesis” postulates that allergic diseases could be prevented by some infections in early childhood. Gammaherpesviruses (γ -HVs) are among the most prevalent human viruses and profoundly imprint on the immune system of their hosts. Using Murid gammaherpesvirus 4 (MuHV-4), a mouse model of human γ -HV infections, we recently showed that γ -HV infection inhibits the development of House Dust Mites (HDM)-induced airway allergy (Machiels et al., *Nature Immunology*, 18(12):1310-1320 (2017)). Group 2 innate lymphoid cells (ILC2s) play a major role in the initiation, maintenance and memory of type 2 immune responses. As activation of these cells can be modulated by viruses associated with asthma exacerbation, we investigated whether MuHV-4 infection affects the lung ILC2s compartment.

1. Gammaherpesvirus infection induces persisting changes in the alveolar niche that protect against airway allergy



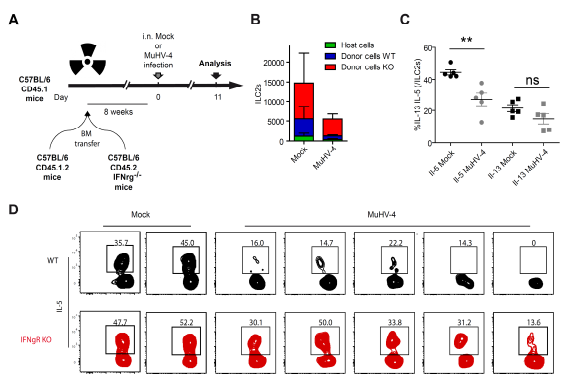
MuHV-4 infection induces persisting changes in alveolar macrophages (AMs) that protect against asthma. In the absence of a previous MuHV-4 infection, resident AMs cannot prevent dendritic cells (DCs) from inducing a strong Th2 response in HDM-induced asthma. MuHV-4 virus infection induces death of AMs and a regulatory phenotype in the infiltrating monocytes that are differentiating into AMs. Long-term-persisting monocyte-derived AMs inhibit HDM-induced asthma by selectively interfering with the ability of DCs to trigger a Th2 response, without affecting Th1 response. The aim of this work is to understand whether MuHV-4 infection and/or recruited immune cells affect lung ILC2s in the context of HDM-induced asthma. Adapted from Bérèngère de Laval & Michael H Sleweke, *Nature Immunology*, News and views, 18(12):1279-1280 (2017).

3. MuHV-4 infection affects activation of ILC2s as revealed by lower expression of PD-1/KLRG1 after HDM sensitization



BALB/c mice (n = 5 to 10 in each group) were infected or not with MuHV-4 and submitted 30 days after infection to HDM sensitization (100 μ g/50 μ L). (A) Representative contour plots of KLRG1 expression on lung ILC2s from the different groups. Numbers in outlined area indicate percent KLRG1+ILC2s. (B) Percentages of KLRG1+ lung ILC2s among the different groups. (C) Representative contour plots of PD-1 expression on lung ILC2s from the different groups. Numbers in outlined area indicate percent PD-1+ILC2s. (D) Percentages of PD-1+ lung ILC2s among the different groups.

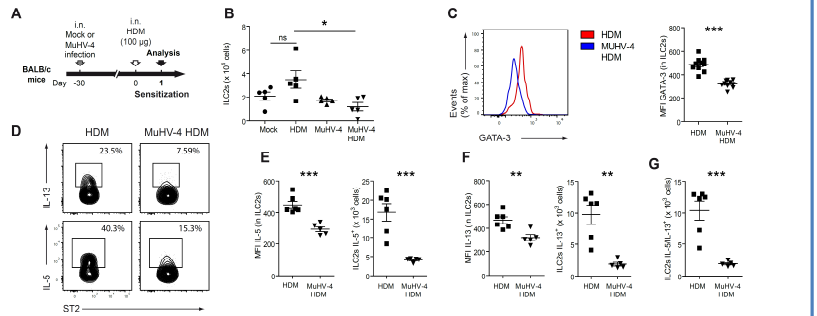
5. IFN- γ production following MuHV-4 infection rapidly modifies ILC2s cytokines production



(A) Experimental model of bone marrow chimeras: CD45.1⁺ BALB/c mice were exposed to lethal irradiation protocol (6Gy). These recipient mice were then given 5 x 10⁶ BM cells isolated from femur and tibia at a ratio of 50% for CD45.1.2⁺ WT and 50% of CD45.2⁺ IFN- γ congenic donors. 8 weeks after BM transfer, these mice were submitted to MuHV-4 infection and analyzed 11 days later (n=5). (B) Representative contour plots for the evaluation of chemerin in lung ILC2s. (C) Percentage production of IL-5 and IL-13 in lung ILC2s and (D) representative contour plots of intracellular stainings of IL-5 on ILC2s, after 4h of ex vivo restimulation with PMA/Ionomycin.

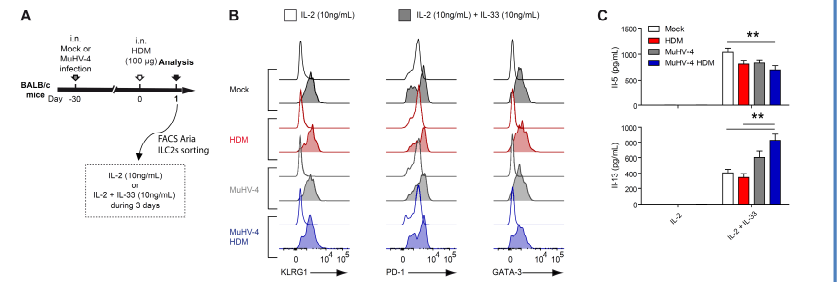
Our results showed that MuHV-4 respiratory infection imprints the function of lung ILC2s following HDM treatment and reduces their capacity to produce type 2 cytokines IL-13 and IL-5. Micro-environment is needed to maintain this phenotype and IFN- γ plays a role in the decrease production of IL-5 cytokine. Single-cell RNA sequencing revealed shared general pattern upon HDM sensitization the presence of a sub-population of ILC2s expressing higher MHC-II in MuHV-4 HDM mice compared to their mock HDM counterparts. These differences may have a determining role in the subsequent development of immune responses against respiratory allergens.

2. MuHV-4 infection affects the function of lung ILC2s after HDM sensitization



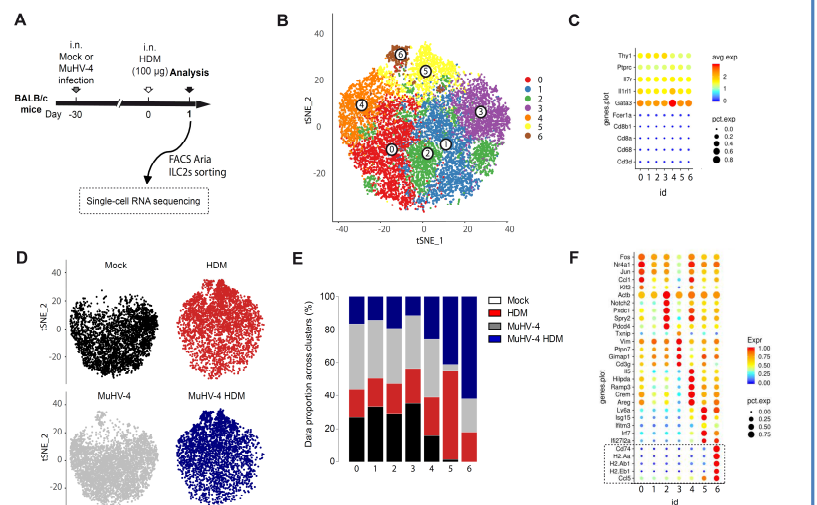
(A) Experimental model of MuHV-4 infection (1.10⁴PFU/50 μ L) and HDM sensitization (100 μ g/50 μ L) in 8-week-old BALB/c mice (n = 6 to 10 in each group). (B) Quantification of lung ILC2s (live Lin CD45⁺CD127⁺CD90.2⁺ST2⁺CD25⁺) cells, after HDM sensitization (lineage markers: B220, CD11c, CD3, CD4, CD49b, CD5, CD8a, F4/80, Fc ϵ R1, Gr1 and Siglec F). (C) Representative histograms and mean fluorescence intensity (MFI) of GATA-3 staining in ILC2s of mice infected or not with MuHV-4 and treated with HDM. (D) Representative contour plots of intracellular stainings of IL-5 and IL-13 on ILC2s isolated from HDM-treated mice, after 4h of ex vivo restimulation with PMA/Ionomycin. (E-F) MFI of IL-5 (E) and IL-13 (F) stainings and numbers of IL-5 (E) and IL-13 (F) producing lung ILC2s after HDM sensitization. (G) Numbers of IL-5 and IL-13 producing ILC2s after HDM sensitization.

4. The reduced activation of lung ILC2s following MuHV-4 infection is not due to an intrinsic defect but is dependent on the microenvironment



(A) Lung ILC2s were sorted from BALB/c mice infected or not with MuHV-4 and submitted 30 days after infection to HDM sensitization (100 μ g/50 μ L), cultured ex-vivo during 3 days with IL-2 or IL-2 + IL-33 (n=6). (B) Representative histograms of KLRG1, PD-1 and GATA-3 expression in sorted ILC2s cultured during 3 days with IL-2 or IL-2 + IL-33. (C) ELISA of cytokines in supernatant of ILC2s cultured during 3 days with IL-2 or IL-2 + IL-33.

6. MuHV-4 infection affects the transcriptional profiles of lung ILC2s clusters



(A) ILC2s were sorted from BALB/c mice infected or not with MuHV-4 (1.10⁴PFU/ 50 μ L) and submitted 30 days after infection to HDM sensitization (100 μ g/50 μ L) (n=6 in each group) and they were profiled by droplet-based single cell RNA-sequencing. ILC2s (defined as Lin CD45⁺CD127⁺CD90.2⁺ST2⁺CD25⁺) cells were sorted after negative enrichment against lineage markers (B220, CD11c, CD3, CD4, CD49b, CD5, CD8a, F4/80, Fc ϵ R1, Gr1 and Siglec F) using MojoSort™ Mouse anti-APC Nanobeads (Biolegend) and magnetic separation using LD columns (Miltenyi) according to the manufacturer's protocol. Gene counts were obtained by aligning reads to the mm10 genome using Cell Ranger software (10x Genomics). (B) t-Distributed stochastic neighbor embedding (t-SNE) plots show 15,846 ILC2s and clustering using top 20 canonical vectors after canonical correlation (CCA) of the 4 conditions. Clusters were named based on the genes that were differentially expressed. (C) Genes expression for markers genes of ILC2s and other immune cell types. (D) t-SNE of ILC2s using top 20 canonical vectors after canonical correlation (CCA) for the 4 conditions. (E) Proportion of treatment condition in each clusters (F) Representative differentially expressed genes (y axis) by clusters and conditions (x axis). Dot size represents the fraction of cells in the cluster that express the gene; color indicates the mean expression (logTPX) in expressing cells, relative to other clusters. Analysis was performed using R package Seurat.